Behavioral Modeling of Complex Magnetic Permeability with High-Order Debye Model and Equivalent Circuits

Xiaokang Liu, Flavia Grassi, *Senior Member, IEEE,* Giordano Spadacini, *Senior Member, IEEE,* Sergio A. Pignari, *Fellow, IEEE,* François Trotti, Nicolas Mora, *Senior Member, IEEE,* and Werner Hirschi

***Abstract*—In this paper, a systematic procedure to derive equivalent circuit networks accurately reproducing the frequency response of the input impedance of magnetic cores in a broad frequency range is presented. The proposed procedure foresees to represent the effective complex permeability spectra of a magnetic core (i.e., the permeability resulting from the superposition of intrinsic material properties and effects due to structural features of the core) by a high-order Debye series expansion, which is subsequently synthesized into suitable Foster and Cauer networks. Such networks can be implemented in any circuit simulator, and are particularly favorable for time-domain transient simulation since they can be easily combined with hysteresis models. Two nanocrystalline tape-wound cores and a commercial bulk current injection probe are used as test cases to prove the effectiveness of the proposed method both in terms of accuracy and ease of implementation.**

***Index Terms*—Complex permeability spectra, Debye models, Foster and Cauer networks, Magnetic components.**

I. Introduction

ACCURATE modeling of the frequency response of magnetic components is of paramount importance in many Electromagnetic Compatibility (EMC) applications, spanning from the selection of suitable common-mode chokes for electromagnetic interference (EMI) filters [1] to the design of magnetic-core probes for testing the immunity of electrical/electronics components, such as those used for susceptibility verification by the bulk current injection (BCI) and pulse current injection (PCI) techniques [2], [3]. In these frameworks, accurate characterization and modeling, through suitable circuit networks, of the frequency response of the magnetic-core complex permeability spectra, is a key ingredient to increase the significance and effectiveness of circuit simulation. Hence, different modeling strategies have been proposed over the past few years to provide accurate circuit representation of magnetic components in a wide frequency interval.

Among these, a first approach is to make use of black-box frequency-dependent models extracted from measurement data [4], [5]. This approach generally provides accurate prediction in the frequency domain but may fail for time-domain transient simulation due to convergence issues and causality problems owing to the inverse *Laplace* transform. A second approach is to resort to single-stage *R-L*, *R-L-C* circuit networks, where the frequency response of the complex permeability is reproduced through an analytical Debye [2] or Lorentz [6] model. This approach allows for overcoming previous limitations, yet generally leading to less accurate prediction, especially in wide frequency intervals. A third approach foresees the use of ladder networks with *R-L* or *R-L-C* components [1], [7]–[10] to fit the measured frequency response. High precision can be achieved through the corresponding representation with suitably-selected stages and parameters. Besides, this approach assures broad applicability both for frequency- and time-domain simulation. However, the process of determining the involved circuit parameters is quite cumbersome. Conventional methods include approximate analytical-expression evaluation [9], [11], whose effectiveness significantly degrades for increasing frequencies, two-step optimization [1], [7], and iterative approximation [8].

In this work, an alternative approach is presented, which foresees the derivation of an analytical high-order Debye model to represent the frequency response of the effective complex permeability spectra of a magnetic core. Model coefficients are extracted through an optimization procedure to identify a suitable set of relaxation frequencies combined with a least-square method [12] to determine the corresponding weight coefficients. In previous papers [12]–[16], similar methods were introduced to provide an analytical representation of intrinsic material properties (i.e., intrinsic permeability/permittivity of magnetic/dielectric materials) to be used for finite-difference time-domain (FDTD) simulation. Conversely, in this work, the obtained Debye representation is used as starting point to synthesize equivalent circuit networks representative for the frequency response of the effective complex permeability spectra, resulting from the superposition of the aforesaid intrinsic material properties and effects pertinent to the specific structure (i.e., shape and dimensions) of the core under analysis, [2], [17]. Particularly, it will be shown that each term of the Debye series can be readily associated with an *R-L* or *R-C* cell in the corresponding Foster network, whose circuit elements are analytically estimated, starting from the pertinent relaxation frequency and weight coefficient. In this respect, it is worth mentioning that the analogy between simplified *R-L-C* networks and Debye and Lorentzian representation of material properties was already outlined in some previous works, e.g., [16], but the objective was not the synthesis of a behavioral model to be exploited for circuit simulation.

For transient simulation (e.g., for pulse current injection), the obtained ladder network can also be converted into the corresponding Cauer I or II networks, and easily combined with advanced hysteresis models [1], [7], [9] accounting for

the nonlinear behavior of the magnetic material. Accuracy and effectiveness of the proposed approach are proven by two application examples, involving two nanocrystalline and ferrite magnetic cores.

The manuscript is organized as follows. In Section II, the procedure to derive the high-order Debye representation of the complex permeability spectra extracted from measurement data is presented. Equivalent circuit networks associated with the obtained Debye models are derived in Section III and IV. In Section V, two application examples, involving magnetic cores with different characteristics, are presented to prove the effectiveness of the proposed modeling strategies. Conclusions are drawn in Section VI.

II. Representation of Complex Permeability Spectra via Debye Models

The frequency response of a magnetic core is determined by the superposition of intrinsic properties of the magnetic material the core is made of (i.e., its intrinsic relative permeability) on the one hand, and effects which are due to its specific structural features (i.e., shape and dimensions) on the other hand. The resulting effective permeability spectra are the quantity of interest in view of circuit simulation of networks in which such a core is arranged as an inductance or a transformer. Unlike measurement of the intrinsic permeability spectra, which requires the use of specific test fixtures as well as availability of suitable material specimens [14], the frequency response of the effective permeability spectra $\hat{\mu}_r(\omega) = \mu'(\omega) - j\mu''(\omega)$ of a magnetic core can be extracted by wounding a wire around the core, and by measuring the resulting input impedance. Once spurious effects introduced by the measurement setup (e.g., effects due to the input connector) have been excluded from the measurement data [18], the resulting impedance $\hat{Z}_{in}$ is written as [7], [18]

$$\hat{Z}_{in}(\omega) = j\omega\hat{L}(\omega) = j\omega L_0\hat{\mu}_r(\omega) \tag{1}$$

where ω denotes the radian frequency and L_0 the theoretical inductance that would be measured assuming that the magnetic field inside the core is ideally distributed. For toroidal cores, an approximate yet valid expression for L_0 is cast as $L_0 = \mu_0 A_c/l_c$ [1], where: μ_0 denotes the free-space permeability, and A_c, l_c are the cross-sectional area and average length of the core, respectively.

A. First-order Debye model

To represent the permeability spectra $\hat{\mu}_r(\omega)$ in (1) through an analytical expression first, and then through a circuit network, the traditional approach is to resort to the first-order Debye model. Accordingly, the frequency response of $\hat{\mu}_r(\omega)$ extracted from the measured input impedance in (1) is fitted by the analytical expression:

$$\hat{\mu}_r(\omega) = \mu_\infty + \frac{\mu_s - \mu_\infty}{1 + j\omega/\omega_0} \tag{2}$$

where μ_s and $\mu_\infty = 1$ denote the core permeability under static conditions, i.e., for $f = 0$ Hz, and for f approaching infinite, respectively. Finally, the radian frequency ω_0 takes the meaning of relaxation frequency.

An example of the frequency response of the first-order Debye model in (2) is plotted in Fig. 1(a), which allows for the circuit representation in Fig. 1(b), whose circuit elements can be readily estimated as:

$$\begin{aligned} L_{eq0} &= L_0 \\ L_{eq1} &= L_0(\mu_s - 1) \\ R_{eq1} &= \omega_0 L_{eq1} \end{aligned} \tag{3}$$

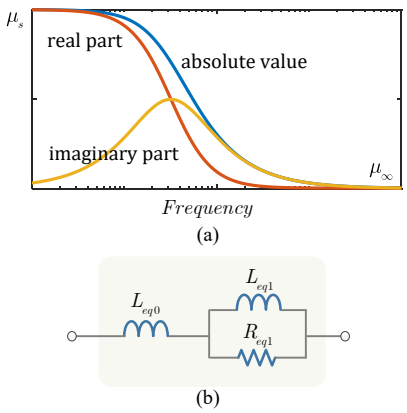

Fig. 1. First-order Debye model: (a) Example of frequency response, and (b) corresponding circuit network.

B. High-order Debye model

The first-order Debye model in (1) often results to be not enough to fit the frequency response of actual magnetic cores, especially in wide frequency intervals, thus making necessary the use of high-order models. To this end, the procedure initially introduced in [12] to extract high-order Debye models of complex dielectric permittivity is here briefly revised with the twofold objective to adapt it to the representation of complex permeability spectra, and to provide them with a suitable circuit representation.

According to [12], the frequency response of the complex permeability $\hat{\mu}_r(\omega)$ in (1) can be accurately reproduced by cascading N_p first-order Debye terms as

$$\hat{\mu}_r(\omega) = \mu_\infty + (\mu_s - \mu_\infty)\sum_{p=1}^{N_p} \frac{a_p}{1 + j\frac{\omega}{\omega_p}} \tag{4}$$

where $\omega_p = 1/\tau_p$ denotes the p-th relaxation frequency with dimensionless weight a_p.

Re-writing $\hat{\mu}_r(\omega)$ as $\hat{\mu}_r(\omega) = \mu'(\omega) - j\mu''(\omega)$, and recognizing that the real $\mu'(\omega)$ and imaginary $\mu''(\omega)$ parts are related via the Kramers-Kronig theory [19], the unknown coefficients of the imaginary part $\mu''(\omega)$ can be fitted as the first step. As a consequence, also the real part is automatically reconstructed by exploiting the very same set of coefficients.

Several global optimization algorithms can be efficiently utilized to extract the set of relaxation frequencies, assuring accurate fitting of $\hat{\mu}_r(\omega)$. In this manuscript, a pattern

search (PS) strategy is utilized for its robustness and ease of implementation in MATLAB. Meanwhile, the least-square (LS) method is used to determine the corresponding weighting vector $\mathbf{a} = [a_1, a_2, \ldots, a_{N_p}]^T$ based on a limited number $N_f \approx 4N_p$ (where N_p usually equals 1-1.5 times the number of frequency decades of interest) of samples of $\mu''(\omega)$. This yields:

$$\mathbf{a} = \left(\mathbf{D}^T\mathbf{D}\right)^{-1}\mathbf{D}^T\mathbf{c} \tag{5}$$

where $\mathbf{c}$ is a $N_f \times 1$ vector with $c_i = \mu''(\omega_i)/(\mu_s - \mu_\infty)$, and $\mathbf{D}$ is a $N_f \times N_p$ matrix with $D_{ip} = \frac{\omega_i}{\omega_p} / \left[1 + \left(\frac{\omega_i}{\omega_p}\right)^2\right]$.

The obtained weights provide the best fit of the frequency response extracted from measurement data in the least-square sense for a given set of relaxation frequencies. The original implementation of the algorithm in [12] foresees the introduction in the Debye series of a compensation term $\Delta\mu$, estimated as the average error between the real part of the expansion and the real part of the actual permeability over all sample frequencies. In the implementation proposed in this work, such compensation is omitted with negligible lack of accuracy, since the objective here is to use the Debye series as the starting point for the synthesis of equivalent circuit networks.

Another noteworthy difference with respect to the original implementation in [12] is concerned with the presence of negative weight coefficients in the Debye series. As a matter of fact, the least-square algorithm can provide one or more negative weight coefficients, which, according to [12], should be discarded (and then compensated) to avoid possible instability of the FDTD solution. Conversely, in this work, the presence of negative weight coefficients is admitted, since this is consistent with the fact that the real part of the complex permeability may become negative in certain frequency intervals. Indeed, the frequency responses measured at the input of actual magnetic cores may exhibit resonances to be ascribed to the combined effect of the intrinsic characteristics of the magnetic material and the specific dimensions of the core under analysis. For this reason, negative weight coefficients are hereinafter retained in the Debye series and provided with a suitable circuit representation (which can be implemented in a whatever circuit simulator without stability issues) in Section IV.

III. Equivalent Circuit Modeling with Positive Weight Coefficients

Under the assumption that all the weight coefficients in (5) are positive, the obtained Debye-series expansion can be transformed into an equivalent circuit network, whose component values can be readily obtained from (5) as explained in this Section.

As the first step, an N_p-stage Foster network, Fig. 2(a) is considered to provide a suitable circuit representation of the core input impedance in (1). Based on the obtained Debye-series expansion, proper inductance and resistance values of the components involved in the Foster network, i.e.:

$$Z_{in}^{Foster} = sL_0^{Foster} + \sum_{p=1}^{N_p}\left(sL_p^{Foster} \parallel R_p^{Foster}\right) \tag{6}$$

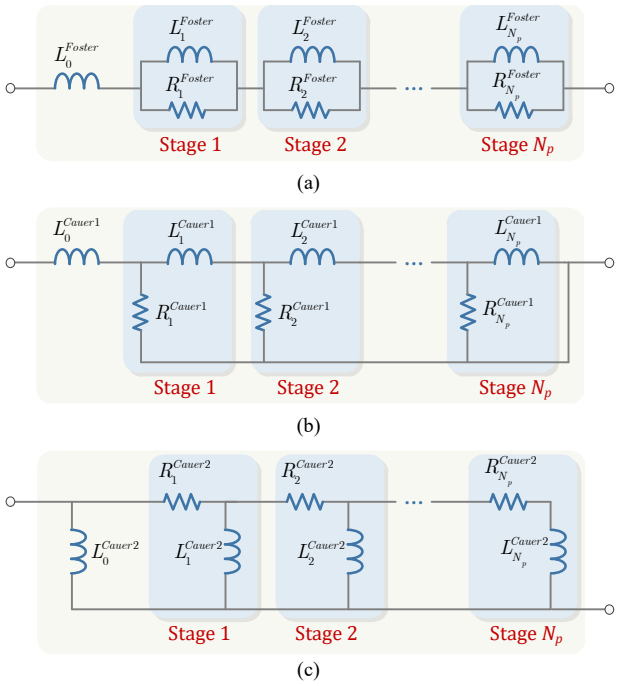

Fig. 2. Equivalent ladder networks used to provide the Debye series expansion in (5) with a suitable circuit representation: (a) Foster; (b) Cauer I; and (c) Cauer II network.

are calculated, by combining the high-order Debye expansion (4) and the complex input impedance expression (1) and (6) (for $p = 1, 2, \ldots, N_p$). This yields:

$$\begin{aligned} L_0^{Foster} &= L_0 \\ L_p^{Foster} &= L_0 a_p (\mu_s - 1) \\ R_p^{Foster} &= \omega_p L_p^{Foster} \end{aligned} \tag{7}$$

Alternative representations can be adopted, such as the Cauer ladder networks in Fig. 2(b) and Fig. 2(c). As a matter of fact, these models result in being more attractive than the Foster one since they can be easily combined with models representative for hysteresis losses (e.g., the Preisach model [9]) so to provide a comprehensive representation of the behavior of magnetic cores for transient time-domain simulation [1], [7].

Suitable values for the *R-L* components involved in the Cauer networks in Fig. 2(b) and Fig. 2(c) are numerically deducted starting from the input impedances Z_{in}^{Cauer1} and Z_{in}^{Cauer2} preliminary cast as the continuous fraction expressions in (8) and (9), respectively.

IV. Equivalent Circuit Modeling in the Presence of Negative Weight Coefficients

As previously mentioned, fitting the input impedance of magnetic cores may involve Debye terms weighted by negative coefficients, since the frequency response of the effective permeability spectra extracted from measurement data may exhibit resonances due to dimensional effects [2], [18]. The presence of negative coefficients in the Debye series requires the introduction of negative-valued components in order to

$$Z_{in}^{Cauer1} = sL_0^{Cauer1} + \cfrac{1}{\frac{1}{R_1^{Cauer1}} + \cfrac{1}{sL_1^{Cauer1} + \cfrac{1}{\frac{1}{R_2^{Cauer1}} + \cfrac{1}{sL_2^{Cauer1} + \cfrac{1}{\ddots + \cfrac{1}{\frac{1}{R_n^{Cauer1}} + sL_n^{Cauer1}}}}}}} \tag{8}$$

$$Z_{in}^{Cauer2} = \cfrac{1}{\frac{1}{sL_0^{Cauer2}} + \cfrac{1}{R_1^{Cauer2} + \cfrac{1}{\frac{1}{sL_1^{Cauer2}} + \cfrac{1}{R_2^{Cauer2} + \cfrac{1}{\frac{1}{sL_2^{Cauer2}} + \cfrac{1}{\ddots + \cfrac{1}{\frac{1}{R_n^{Cauer2}} + sL_n^{Cauer2}}}}}}}} \tag{9}$$

synthesize an equivalent network accurately reproducing the actual frequency response, [20].

Let's suppose that the obtained Debye series involves a negative weight coefficient. This should theoretically reflect into a negative-valued *R-L* parallel cell in the corresponding Foster network. In order to reduce the number of negative circuit elements to the minimum, such a cell can be equivalently modeled as illustrated in Fig. 3, which is a positive-valued *R-C* parallel cell connected in series with a negative-valued resistor *R*, [20]. Assuming the negative weight and its corresponding relaxation frequency to be a_n and ω_n, respectively, suitable values for the involved *R* and *C* components are given by the expressions:

$$\begin{aligned} R &= -a_n \omega_n L_0 \left(\mu_s - 1\right) \\ C &= \frac{1}{\omega_n R} = \frac{1}{-a_n \omega_n^2 L_0 (\mu_s - 1)} \end{aligned} \tag{10}$$

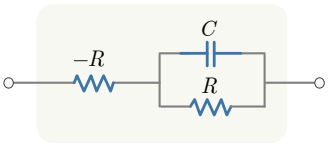

Fig. 3. Equivalent circuit representation of a term of the Debye series weighed by a negative coefficient.

The procedure can be generalized for whatever number of negative weight coefficients. For instance, if the obtained Debye series involves M positive and N negative weight coefficients, the corresponding input impedance can be modelled by the Foster network depicted in Fig. 4, which was obtained by connecting in series (a) the initial series inductance L_0; (b) N negative resistors and N (positive-valued) *R-C* cells associated with the N negative weight coefficients; (c) M (positive-valued) *R-L* cells associated with the M positive weight coefficients. In spite of the presence of a negative-valued resistor, the real part of the impedance associated with the elemental cell in Fig. 3 is positive. Hence, on condition the number of relaxation frequencies was properly selected, this representation assures that also the real part of the input impedance of the core takes positive value.

V. Application Examples

In this Section, two application examples are presented to validate and prove the effectiveness of the proposed modeling procedure, both in the absence and in the presence of negative weight coefficients. Eventually, time-domain measurements are presented to assess the prediction accuracy of the proposed core model for time-domain simulation.

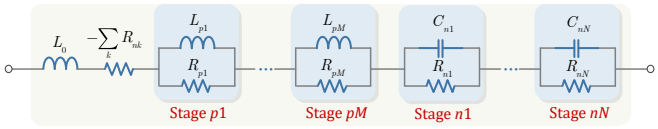

Fig. 4. Equivalent Foster network for the synthesis of an input impedance fitted by a Debye series with M positive and N negative weight coefficients.

A. Model validation in the absence of negative weight coefficients

The first two examples do not involve negative coefficients and illustrate the measurement and modelling of the frequency response of the complex relative permeability spectra of two nanocrystalline magnetic cores made of Vitroperm material [21], [22], as shown in Fig. 5(a).

The geometrical characteristics of the cores under analysis are: cross-sectional area $A_c = 2.28$ / 1.62 cm^2, average length $l_c = 23.6$ / 22.5 cm (for W984 and W436, respectively). For experimental characterization, a thin conductive tape was wound around the core, and the extremities were soldered to the inner pin, and outer shield of an N-type and a subminiature version A (SMA)-type connector [see Fig. 5(a)]. The core input impedances were measured by a Vector Network Analyzer in the frequency interval from 10 kHz up to 1 GHz, and the spurious effects introduced by input connectors were then removed from measurement data, according to [18]. Based on the obtained results, the complex permeability spectra of the cores were retrieved by means of (1). Also, input impedance measurements allowed estimating the initial permeabilities of the two cores as $\mu_s = 3,400$ and $20,000$, which are in line with the specifications provided by the manufacturer.

By application of the proposed algorithm, the core input impedances were satisfactorily fitted by third-order Debye series, involving positive coefficients only. For the core W436, the corresponding circuit networks are shown in Fig. 6, whose *R-L* values, estimated through the procedure proposed in Section III, are collected in Tab. I. Similar circuits (not reported here for brevity) are also obtained for the second core, whose *R-L* values are collected in Tab. II. The comparisons between the complex relative permeability spectra obtained from

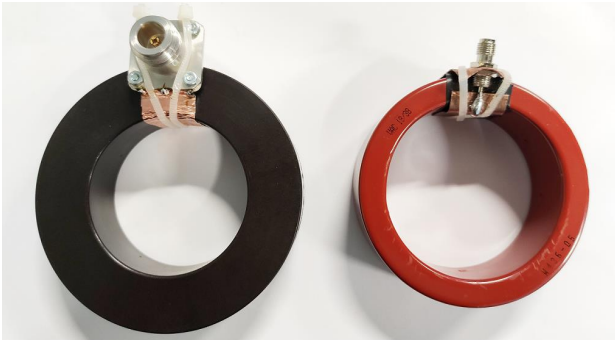

(a)

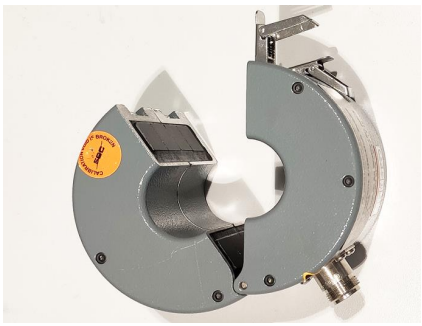

(b)

Fig. 5. Pictures of the two magnetic components characterized and modeled by the proposed technique: (a) Nanocrystalline magnetic core Vacuumschmelze W984 (left) and W436 (right) with hand-made injection connector and winding; and (b) a commercial BCI probe FCC F-130A.

TABLE I
MODEL PARAMETERS FOR NANOCRYSTALLINE CORE W436

Model	Param.	Stage 0	Stage 1	Stage 2	Stage 3
Debye*	ω_p [rad]		1.2548E6	1.0211E7	8.0031E7
	a_p		0.7786	0.1488	0.0680
Foster	L [H]	9.0478E-10	1.3707E-5	2.8368E-6	1.1661E-6
	R [Ω]		17.1997	28.9658	93.3258
Cauer I	L [H]	9.0478E-10	2.4990E-6	5.8628E-6	9.3486E-6
	R [Ω]		139.4914	53.3314	18.8784
Cauer II	L [H]	1.7711E-5	4.0640E-6	1.1509E-6	9.0574E-10
	R [Ω]		27.9663	46.9979	64.6928

* Initial permeability of the Debye model: $\mu_s = 20,000$.

measurement data and those reconstructed by the proposed model(s) are shown in Fig. 7, and shows good agreement in the frequency interval from 10 kHz up to 1 GHz.

B. Model validation in the presence of negative weight coefficients

As an application example of the proposed procedure in the presence of negative weight coefficients, experimental characterization and modeling of the complex permeability spectra of the ferrite core of a commercial injection probe for BCI immunity testing (i.e., probe FCC F-130A [18]) is addressed in this subsection [see Fig. 5(b)]. For this probe, the main geometrical and electrical characteristics, as well as a detailed description of the procedure used to extract the spectra of complex permeability from input impedance measurement

TABLE II
MODEL PARAMETERS FOR NANOCRYSTALLINE CORE W984

Model	Param.	Stage 0	Stage 1	Stage 2	Stage 3
Debye*	ω_p [rad]		7.1131E6	6.6020E7	3.4955E8
	a_p		0.8072	0.1069	0.0891
Foster	L [H]	1.2140E-9	3.3309E-6	4.4092E-7	3.6778E-7
	R [Ω]		23.6931	29.1095	128.5565
Cauer I	L [H]	1.2140E-9	6.9941E-7	1.1842E-6	2.2560E-6
	R [Ω]		181.3591	54.1558	31.2281
Cauer II	L [H]	4.1408E-6	8.4888E-7	3.3145E-7	1.2206E-9
	R [Ω]		36.0212	77.4090	68.9574

* Initial permeability for the Debye model is $\mu_s = 3,400$.

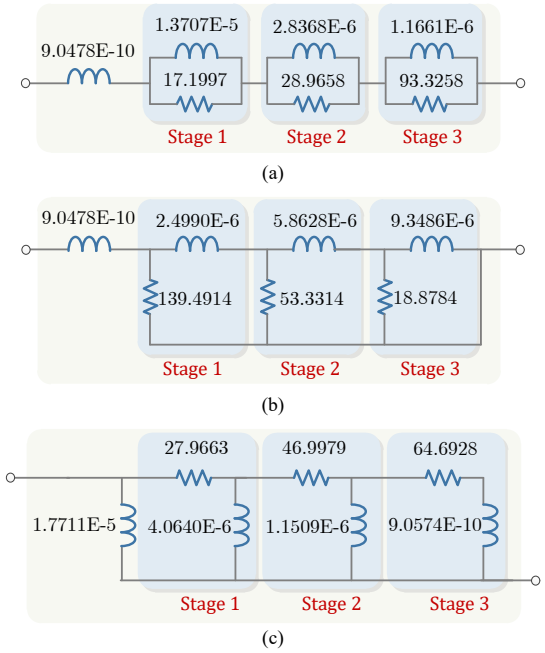

Fig. 6. Ladder circuit networks used to model the frequency response of the input impedance of the Vacuumschmelze W436 core: (a) Foster, (b) Cauer I and (c) Cauer II network.

data can be found in [18], and therefore not repeated here for brevity.

As observed in that work, the combined effects due intrinsic material properties superimposed to dimensional/structural resonances and eddy currents introduce a pronounced resonance phenomenon in the frequency response of such a probe, giving rise to negative weight coefficients in the Debye series. Particularly, in the frequency interval from 300 kHz up to 400 MHz, it is found that the proposed procedure assures accurate fitting of the pertinent permeability spectra by means of a 5-th order Debye model involving one negative weight coefficient (see Table III). The corresponding Foster network is shown in Fig. 8. The complex permeability spectra obtained from input impedance measurement and those reconstructed by the proposed 5-th order Debye model is shown in Fig. 9. The achieved agreement proves the effectiveness and accuracy of the proposed method.

It is worth mentioning that the number of used terms of the Debye series here is higher than in the previous examples,

TABLE III
MODEL PARAMETERS FOR FCC F-130A

Model	Param.	Stage 0	Stage 1	Stage 2	Stage 3	Stage 4	Stage 5
Debye*	ω_p [rad]		2.1418E6	3.3325E7	4.8534E8	4.8599E8	4.8713E8
	a_p		0.2306	0.2520	1.2453E5	-1.9600E5	7.1461E4
Foster**	L [H]	4.8551E-9	4.8934E-7	5.3463E-7	0.2642	–	0.1516
	R [Ω]	-2.0209E8	1.0480	17.8164	1.2824E8	2.0209E8	7.3858E7
	C [F]	–	–	–	–	1.0182E-17	–

* Initial permeability for the Debye model is $\mu_s = 438$.

** Stage 0: L/R components are in series.

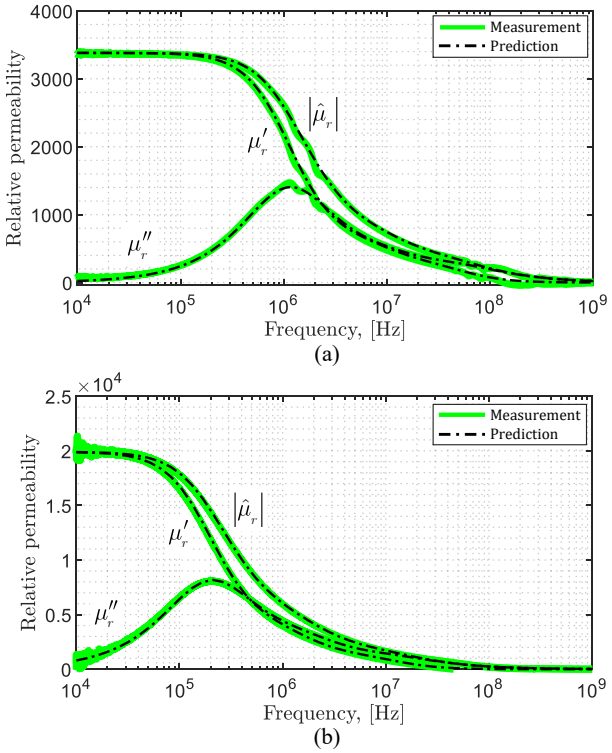

Fig. 7. 3-rd order Debye model fitting the complex permeability spectra of the Vacuumschmelze (a) W984 core and (b) W436 core: Measurement data (solid curves) versus reconstructions (dash-dotted curves).

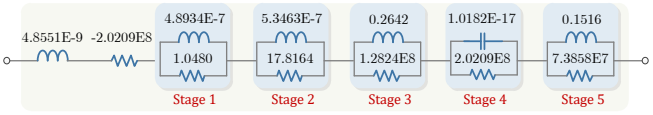

Fig. 8. Foster network modelling the frequency response of the input impedance of the BCI probe FCC F-130A.

even though the frequency interval of interest is limited to 500 MHz only. This is due to the presence of negative coefficients. Indeed, in this case, it is possible that the real part of the overall impedance, which corresponds to the imaginary part of the effective permeability in (1), may become negative, with consequent convergence issues for time-domain simulation. This can be easily avoided by increasing the number of relaxation frequencies (i.e., the order of the Debye series) until the frequency response of the real part does not longer exhibit

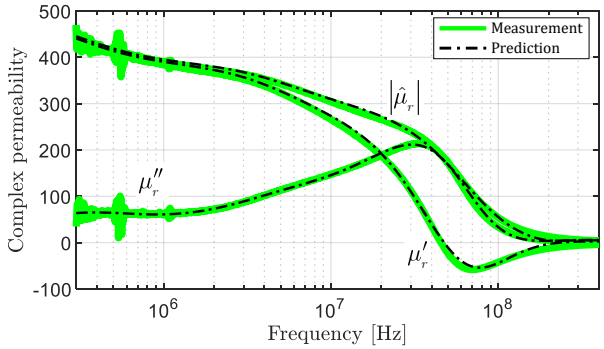

Fig. 9. 5-th order Debye model fitting the complex permeability spectra of the BCI probe FCC F-130A: Measurement data (solid curves) versus reconstructions (dash-dotted curves).

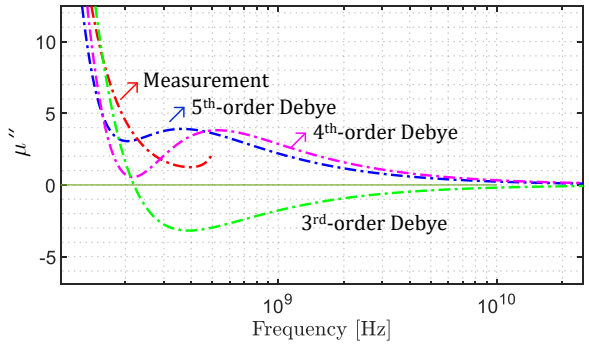

Fig. 10. BCI probe FCC F-130A: Frequency response of the imaginary part of the complex permeability reconstructed by the proposed algorithm for different orders of the Debye series.

negative values. For the specific example here considered (i.e., FCC F-130A probe), in Fig. 10 the imaginary parts of the complex permeability spectra evaluated for increasing number of relaxation frequencies (i.e., fitted through a third, fourth and fifth-order Debye model) are compared in the interval from 100 MHz up to 30 GHz. The comparison clearly shows that (unlike measurement data) the reconstruction obtained resorting to a third-order approximation exhibits negative values for frequencies above 200 MHz. This does no longer occur for higher-order Debye approximations (as the fifth-order model used in Fig. 9), thus assuring simulation convergence.

C. Validation by time-domain measurement

To assess the effectiveness of the model also for time-domain simulations, the test setup in Fig. 11 was used. The setup involves the nanocrystalline core W436 mounted at the midpoint of a hand-made calibration fixture, that was previously modeled as in [18]. The input connector of the nanocrystalline core is connected to the 50 Ω output of an arbitrary waveform generator (AWG) Keysight M8190A, which is used to generate Gaussian pulses with different center frequencies. The induced voltage waveforms at the right end of the calibration fixture were measured by a 50 Ω oscilloscope, and the other fixture end was terminated in a 50 Ω load.

The peak-to-peak amplitude (i.e., 700 mV) of the injected waveform was kept to a significantly lower value than the core saturation level. Moreover, since the nanocrystalline core is characterized by extremely-low hysteresis losses w.r.t. Eddy-current losses, the proposed small-signal model is expected to assure accurate reproduction of the core frequency response, without the need for including any nonlinear effect, as in [7], [9].

For time-domain simulation of the mentioned setup (see Fig. 12), the proposed circuit model of the nanocrystalline core was combined with a distributed-parameter model of the calibration fixture, [4], [18]. A Thevenin equivalent was used to represent the AWG in the circuit simulation. It corresponds to a 50 Ω resistor in series with an ideal voltage source retrieved from the voltage measured on the second AWG channel. Results obtained for Gaussian pulses with center frequencies of 100 kHz and 1 MHz are shown in Fig. 13. The good agreement between the waveforms predicted by the proposed model in Fig. 12 (dash-dotted curves) and the actual waveforms measured at the fixture right-end (solid curves) confirms the effectiveness and accuracy of the proposed modeling technique also for time-domain simulation. For the sake of comparison, also the predictions obtained by modelling the core by a constant-valued inductance, corresponding to the first term of the Debye series expansion, are shown (dotted curves).

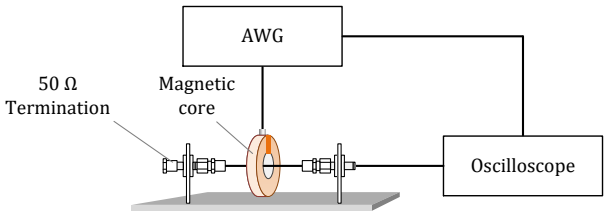

(a)

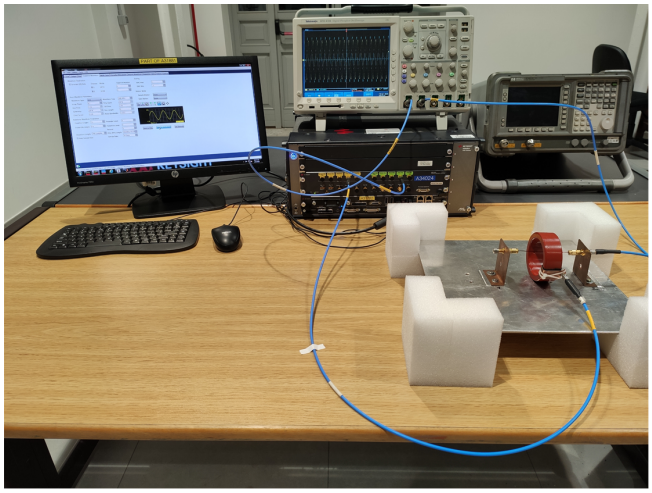

(b)

Fig. 11. (a) Principle drawing and (b) test setup for validating the model of the nanocrystalline core W436 by time-domain measurement.

VI. Conclusion

In this work, a systematic approach aimed at determining equivalent circuits for reproducing the frequency response of the input impedance of magnetic components in a wide frequency interval was presented. The method foresees to preliminarily fit the complex spectra of magnetic permeability extracted from measurement data by an analytical high-order Debye series. The obtained series is afterward converted into an equivalent ladder Foster/Cauer network, whose *R-L* and/or *R-C* cells are uniquely associated with each term in the Debye series. Simple rules to determine the values of the involved *R*, *L*, *C* components are provided starting from the Debye series involving not only positive but also negative weight coefficients (which occurs when the frequency response to be fitted exhibits resonances). Compared with previous methods, the proposed technique assures high accuracy along with a significant reduction of computational efforts. Namely, it only requires a single-step optimization procedure to determine a suitable set of relaxation frequencies, followed by a least-square method based on a limited number of samples to evaluate the corresponding weight coefficients. The obtained ladder networks can be implemented in a whatever circuit simulator and used for simulation not only in the frequency but also in the time domain, where applicable combined with hysteresis models [1], [7], [9].

References

[1] A. Muetze and C. R. Sullivan, "Simplified design of common-mode chokes for reduction of motor ground currents in inverter drives," *IEEE Trans. Ind. Appl.*, vol. 47, no. 6, pp. 2570–2577, 2011.

[2] N. Toscani, F. Grassi, G. Spadacini, and S. A. Pignari, "Circuit and electromagnetic modeling of bulk current injection test setups involving complex wiring harnesses," *IEEE Trans. Electromagn. Compat.*, vol. 60, no. 6, pp. 1752–1760, 2018.

[3] X. Liu, L. Crosta, F. Grassi, G. Spadacini, S. A. Pignari, F. Trotti, N. Mora, and W. Hirschi, "SPICE Modeling of Probes for Pulse Current Injection," in *Proc. IEEE ESA Workshop Aerosp. EMC*, May 2019, pp. 1–6.

[4] F. Grassi, F. Marliani, S. A. Pignari *et al.*, "SPICE modeling of BCI probes accounting for the frequency-dependent behavior of the ferrite core," in *Proc. 19th URSI Gen. Assem.*, Chicago, IL, USA, Aug. 2008, pp. 1–4.

[5] K. Nomura, N. Kikuchi, Y. Watanabe, S. Inoue, and Y. Hattori, "Novel SPICE model for common mode choke including complex permeability," in *Proc. IEEE Appl. Power Electron. Conf. Expo. (APEC)*, Mar. 2016, pp. 3146–3152.

[6] S. Miropolsky, S. Frei, and J. Frensch, "Modeling of bulk current injection (BCI) setups for virtual automotive IC tests," in *Proc. EMC Europe*, Wroclaw, Poland, Sep. 2010, pp. 1–6.

[7] C. R. Sullivan and A. Muetze, "Simulation model of common-mode chokes for high-power applications," *IEEE Trans. Ind. Appl.*, vol. 46, no. 2, pp. 884–891, 2010.

[8] K. Nomura, T. Kojima, and Y. Hattori, "Straightforward modeling of complex permeability for common mode chokes," *IEEJ Journal of Industry Applications*, vol. 7, no. 6, pp. 462–472, 2018.

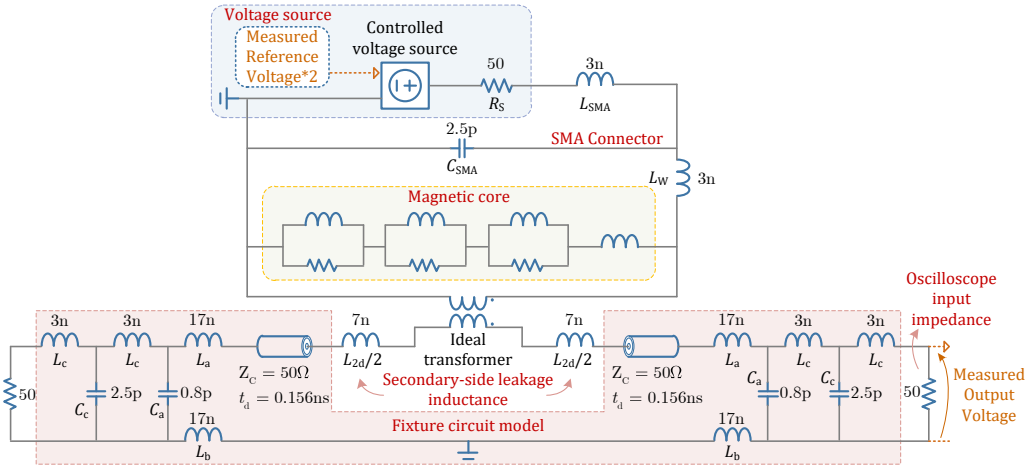

Fig. 12. Schematics for time-domain simulation of the measurement setup in Fig. 11. Here, the proposed third order Foster network is used for modeling the magnetic core, yet alternative implementations based on Cauer networks are possible.

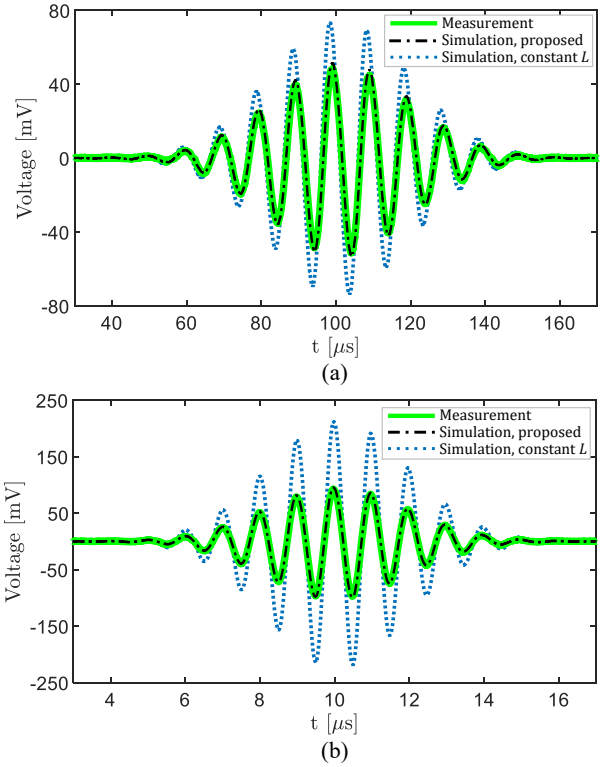

Fig. 13. Measurement (solid curves) versus prediction (dash-dotted and dotted curves) of the waveforms induced at one termination of the fixture in Fig. 11, for two Gaussian pulses with fractional bandwidth 0.2 and centered at (a) 100 kHz and (b) 1 MHz, respectively, injected at the input port of the nanocrystalline core under analysis.

[9] B. Wunsch, S. Skibin, V. Forsstrom, and T. Christen, "Broadband modeling of magnetic components with saturation and hysteresis for circuit simulations of power converters," *IEEE Trans. Magn.*, vol. 54, no. 11, pp. 1–5, 2018.

[10] H. Zhu, D. Liu, H. Chen, and G. Chen, "An improved foster model of common-mode inductor and its application in EMI filter design," in *Proc. IEEE Joint Int. Symp. Electromagn. Compat. Asia–Pacific Int. Symp. Electromagn. Compat. (EMC/APEMC)*, May 2018, pp. 461–465.

[11] P. Holmberg, A. Bergqvist, and G. Engdahl, "Modelling eddy currents and hysteresis in a transformer laminate," *IEEE Trans. Magn.*, vol. 33, no. 2, pp. 1306–1309, 1997.

[12] D. F. Kelley, T. J. Destan, and R. J. Luebbers, "Debye function expansions of complex permittivity using a hybrid particle swarm-least squares optimization approach," *IEEE Trans. Antennas Propag.*, vol. 55, no. 7, pp. 1999–2005, 2007.

[13] M. Y. Koledintseva, J. Wu, H. Zhang, J. L. Drewniak, and K. N. Rozanov, "Representation of permittivity for multi-phase dielectric mixtures in FDTD modeling," in *Proc. IEEE Int. Symp. Electromag. Compat*, vol. 1, Santa Clara, CA, Aug. 2004, pp. 309–314.

[14] J. Xu, M. Y. Koledintseva, Y. He, R. E. DuBroff, J. L. Drewniak, B. Matlin, and A. Orlando, "Measurement of electromagnetic parameters and FDTD modeling of ferrite cores," in *Proc. IEEE Int. Symp. Electromagn. Compat.*, Aug. 2009, pp. 83–88.

[15] S. Jing, Y.-J. Zhang, J. Li, D. Liu, M. Y. Koledintseva, D. J. Pommerenke, J. Fan, and J. L. Drewniak, "Extraction of permittivity and permeability for ferrites and flexible magnetodielectric materials using a genetic algorithm," *IEEE Trans. Electromagn. Compat.*, vol. 57, no. 3, pp. 349–356, 2015.

[16] M. Y. Koledintseva, J. L. Drewniak, D. J. Pommerenke, G. Antonini, A. Orlandi, and K. N. Rozanov, "Wide-band Lorentzian media in the FDTD algorithm," *IEEE Trans. Electromagn. Compat.*, vol. 47, no. 2, pp. 392–399, 2005.

[17] G. R. Skutt, "High-frequency dimensional effects in ferrite-core magnetic devices," Ph.D. Dissertation, Virginia Polytech. Inst., State Univ.,, Blacksburg, 1996.

[18] F. Grassi, F. Marliani, and S. A. Pignari, "Circuit modeling of injection probes for bulk current injection," *IEEE Trans. Electromagn. Compat.*, vol. 49, no. 3, pp. 563–576, Aug. 2007.

[19] C. A. Balanis, *Advanced Engineering Electromagnetics*. New York: John Willey & Sons Inc., 1989.

[20] W. Tan, C. Cuellar, X. Margueron, and N. Idir, "A high frequency equivalent circuit and parameter extraction procedure for common mode choke in the EMI filter," *IEEE Trans. Power Electron.*, vol. 28, no. 3, pp. 1157–1166, 2012.

[21] Vacuumschmelze, "Specification for Soft Magnetic Cores (VAC L2090-W984-02)," https://www.vacuumschmelze.com/Assets-Web/984-02-%281%29.pdf, (Accessed Aug. 3, 2020).

[22] Vacuumschmelze, "Specification for Soft Magnetic Cores (VAC W436-05 JJKW)," https://vacuumschmelze.com/Assets-Web/L2080-W436_en_de.pdf, (Accessed Aug. 3, 2020).

Xiaokang Liu received the double M.Sc. degree in electrical engineering from Xi'an Jiaotong University, Shaanxi, China, and Politecnico di Milano, Milan, Italy, in 2016. Since November 2017, he has been working toward the Ph.D. degree in electrical engineering at Politecnico di Milano.

His research interests include electromagnetic compatibility, power electronics and signal integrity.

Flavia Grassi (M'07-SM'13) received the Laurea (M.Sc.) and Ph.D. degrees in electrical engineering from Politecnico di Milano, Milan, Italy, in 2002 and 2006, respectively.

She is currently an Associate Professor in the Department of Electronics, Information and Bioengineering, Politecnico di Milano. From 2008 to 2009, she was with the European Space Agency (ESA), ESA/ESTEC, The Netherlands, as a Research Fellow. Her research interests include distributed-parameter circuit modeling, statistical techniques, characterization of measurement setups for EMC testing (aerospace and automotive sectors), and application of the powerline communications technology in ac and dc lines.

Dr. Grassi received the International Union of Radio Science (URSI) Young Scientist Award in 2008, and the IEEE Young Scientist Award at the 2016 Asia- Pacific International Symposium on EMC (APEMC), the IEEE EMC Society 2016 Transactions Prize Paper Award, and the Best Symposium Paper Award at the 2015 and 2018 APEMC.

Giordano Spadacini (M'07–SM'16) received the Laurea (M.Sc.) and Ph.D. degrees in electrical engineering in 2001 and 2005, respectively, from Politecnico di Milano, Italy, where he is currently an Associate Professor with the Dept. of Electronics, Information and Bioengineering. His research interests include statistical models for the characterization of interference effects, distributed parameter circuit modeling, experimental procedures and setups for EMC testing, and EMC in aerospace, automotive and railway systems.

Dr. Spadacini is a recipient of the 2005 EMC Transactions Prize Paper Award, the 2016 Richard B. Schulz Best EMC Transactions Paper Award, two Best Symposium Paper Awards from the 2015 Asia-Pacific Int. Symp. on EMC (APEMC) and the 2018 Joint IEEE EMC & APEMC Symposium.

Sergio A. Pignari (M'01–SM'07–F'12) received the Laurea (M.S.) and Ph.D. degrees in electronic engineering from Politecnico di Torino, Turin, Italy, in 1988 and 1993, respectively.

From 1991 to 1998, he was an Assistant Professor with the Dept. of Electronics, Politecnico di Torino, Turin, Italy. In 1998, he joined Politecnico di Milano, Milan, Italy, where he is currently a Full Professor of Circuit Theory and Electromagnetic Compatibility (EMC) at the Dept. of Electronics, Information, and Bioengineering, and Chair of the board of B.Sc. and M.Sc. Study Programmes in Electrical Engineering, term 2015-20. He is the author or coauthor of more than 200 papers published in international journals and conference proceedings. His research interests are in the field of EMC and include field-to-wire coupling and crosstalk, conducted immunity and emissions in multi-wire structures, statistical techniques for EMC prediction, and experimental procedures and setups for EMC testing.

Dr. Pignari is co-recipient of the 2005 and 2016 IEEE EMC Society Transactions Prize Paper Award, and a 2011 IEEE EMC Society Technical Achievement Award. He is currently serving as an Associate Editor of the IEEE TRANSACTIONS ON ELECTROMAGNETIC COMPATIBILITY. From 2010 to 2015 he served as the IEEE EMC Society Chapter Coordinator. From 2007 to 2009 he was the Chair of the IEEE Italy Section EMC Society Chapter. He has been Technical Program Chair of the ESA Workshop on Aerospace EMC since 2009, and a Member of the Technical Program Committee of the Asia Pacific EMC Week since 2010. He is a member of the International Academic Committee of The State Key Laboratory of Electrical Insulation and Power Equipment (SKLEIPE) at Xi'an Jiaotong University (XJTU), Xi'an, China, term 2015-20.

François Trotti has studied electrical engineering at the EPFL in Lausanne, Switzerland. He worked 8 years at ABB in Turgi in the development of power converter for traction application and acted as project manager for testing the traction converter for the SBB locomotive Re 460 "loco 2000". In 1995, he joined the EMC test laboratory EMC Fribourg (later montena emc). Today he is active as development engineer and project manager for NEMP and other pulse generators at montena technology in Rossens.

Nicolas Mora (M'07–SM'18) was born in Bogota, Colombia. He received a B. S. degree in Electronics Engineering in 2007, and a M.Sc. degree in Electrical Engineering with a major in High Voltage Engineering in 2009, both from the National University of Colombia. He joined the EMC Research Group of the National University of Colombia in 2007. In 2009 he joined the EMC Lab at the Swiss Federal Institute of Technology (EPFL). He received his Ph. D degree in Electrical Engineering from EPFL in 2016. From 2015 to 2019 he worked as an R & D Engineer for montena technology. In 2020 he joined the Directed Energy Research Center of the Technology Innovation Institute in Abu Dhabi.

In 2011, he received the Frank Gunther Award of the Radio Club of America and the Young Scientist Award from URSI. From 2013-2016, Nicolas was the president of the Colombian Association of Researchers in Switzerland. In 2015 he received the Young Scientist Award from the Summa Foundation. He was appointed as a Distinguished Reviewer of the IEEE TRANSACTIONS ON ELECTROMAGNETIC COMPATIBILITY in 2015, 2016, 2018 and 2019. He was the chair of the joint EMC / AP / MTT chapter of IEEE in Switzerland between 2016 and 2019. In 2016, he received the Best Paper Award from the EMC Europe 2016 Wroclaw Symposium. In 2018, he received the HPEM Fellow award from the Summa Foundation, and in 2019 the Motohisa Kanda Most Cited IEEE Transactions in EMC Paper Award.

Werner Hirschi has studied Electrical Engineering at the ”Ecole d’Ingénieurs”, in Fribourg, Switzerland. Over the years he has worked in all areas of EMC engineering. Today, his activity is mainly focused on simulation of electromagnetic threats and detection of electromagnetic attacks.
W. Hirschi is CEO of montena technology sa.